Helicity Observation of Weak and Strong Fields

Mei Zhang[1]

ABSTRACT

We report in this letter our analysis of a large sample of photospheric vector magnetic field measurements. Our sample consists of 17200 vector magnetograms obtained from January 1997 to August 2004 by Huairou Solar Observing Station of the Chinese National Astronomical Observatory. Two physical quantities, α and current helicity, are calculated and their signs and amplitudes are studied in a search for solar cycle variations. Different from other studies of the same type, we calculate these quantities for weak ($100G < |B_z| < 500G$) and strong ($|B_z| > 1000G$) fields separately. For weak fields, we find that the signs of both α and current helicity are consistent with the established hemispheric rule during most years of the solar cycle and their magnitudes show a rough tendency of decreasing with the development of solar cycle. Analysis of strong fields gives an interesting result: Both α and current helicity present a sign opposite to that of weak fields. Implications of these observations on dynamo theory and helicity production are also briefly discussed.

Subject headings: MHD — Sun: magnetic fields — Sun: interior

1. Introduction

Magnetic helicity is a physical quantity that measures the topological complexity of a magnetic field, such as the degree of linkage and/or twistedness in the field (Moffatt 1985, Berger & Field 1984). It has been shown that its total amount is approximately conserved in the Sun even when there is an energy release during fast magnetic reconnection (Berger 1984). This conservation of total magnetic helicity is considered to play an important role in the dynamical processes in the Sun. For example, by considering helicity conservation in the mean-field dynamo, theories have predicted that solar dynamo would produce opposite helicity signs in the mean field and in the fluctuations (Blackman & Field 2000, see Ossendrijver

[1]National Astronomical Observatory, Chinese Academy of Sciences, A20 Datun Road, Chaoyang District, Beijing 100012, China; Email: zhangmei@bao.ac.cn

2003 for a review). It has also been considered that magnetic helicity and its conservation may play an important role in CME dynamics (Low 2001, Demoulin et al. 2002) where accumulation of total magnetic helicity in the respective northern and southern hemispheres leads to a natural magnetic energy storage for CME eruptions (Zhang & Low 2005, Zhang, Flyer & Low 2006).

A direct measurement of magnetic helicity and hence a direct test of above theories by observations are still out of our reach because so far the photosphere is still the only layer that we can measure vector magnetic fields with reasonable temporal and spatial resolutions. However, by calculating derived physical quantities, such as α and current helicity, from observed photospheric vector magnetograms we do get a glimpse of properties of magnetic helicity in the Sun. For example, from photospheric magnetic field measurements we learn that magnetic fields emerging from the solar convection zone to the photosphere are already significantly twisted (Kurokawa 1987, Leka et al. 1996) and statistically these fields possess a positive helicity sign in the southern hemisphere and a negative helicity sign in the northern hemisphere (Pevtsov et al. 1995, Bao & Zhang 1998). These observations thus provide us implications on how magnetic helicity might be produced in the convection zone (Berger & Ruzmaikin 2000) and how magnetic helicity conservation might have played a role in balancing the twist and writhe helicity in an originally untwisted flux rope (Longcope et al. 1998).

In this letter, we intend to use photospheric vector magnetic field measurements to find further observational indications of helicity production and conservation. Different from other works of the same type, we separate studied fields into two parts: strong magnetic fields and weak magnetic fields. We organize our paper as follows: In §2, we describe our observation and data reduction. In §3, we present our analysis and discussions. We conclude the letter with a brief summary in §4.

2. Observation and Data Reduction

The tunable birefringent filter of the solar telescope magnetograph at the Huairou Solar Observing Station of the Chinese National Astronomical Observatory can be aimed at different passbands for different observations (Ai & Hu 1986). For photospheric observations the passband of the filter is set in the FeIλ5324 line: at 0.075Å from the line center for the measurement of longitudinal magnetic field (Stokes V) and at the line center for the measurement of transverse magnetic fields (Stokes Q and U). More information of the magnetograph and calibration can be found in Ai et al. (1982) and Zhang & Ai (1986).

A dataset of photospheric vector magnetograms obtained by above magnetograph during the period of 1997 January 1 to 2004 August 31 is analyzed in this letter. This dataset contains 17200 vector magnetograms and covers almost all active regions appeared during this period. We calibrate each vector magnetogram according to Ai et al. (1982) and solve the 180-degree ambiguity by setting the directions of transverse fields most closely to a current-free field.

We calculate two physical quantities, α and current helicity, of each magnetogram, as helicity proxies. We calculate α, either as a best-fit single value α_{best} following Pevtsov et al. (1995) or as a mean value $\langle\alpha_z\rangle$ of the local $\alpha_z = (\nabla \times \mathbf{B})_z/B_z$ as in Pevtsov et al. (1994). The two α values so calculated are all indicators of the twistedness of the measured field and there is a linear relationship between them when derived from the same set of magnetograms (Burnette et al. 2004). We shall use α_{best} in §3.1 in comparison with Pevtsov et al. (2001) and $\langle\alpha_z\rangle$ in §3.2 and §3.3 for $\langle\alpha_z\rangle$ is presumably less dependent on the linear force-free assumption. The current helicity is calculated as $h_c = B_z \cdot (\nabla \times \mathbf{B})_z$, which is actually the longitudinal (z) component of the current helicity density at the photosphere ($z = 0$). When calculating these quantities we have used only those magnetograms whose longitudes are less than 40 degrees from the disk center and only those data points whose longitudinal flux densities ($|B_z|$), after the correction of projection effect, are greater than 100G and whose transverse flux densities ($|B_x|$ and $|B_y|$) are both greater than 200G. Note our treatments in data reduction so far are as typical as most other authors in reducing vector magnetograms (Pevtsov et al., 1994, 1995, 2001; Bao & Zhang 1998).

Our unique treatment of the data is that we divide our studied fields into two parts: strong magnetic fields whose longitudinal flux densities ($|B_z|$) are greater than 1000G, and weak magnetic fields whose longitudinal flux densities ($|B_z|$) are between 100G and 500G. By such a definition, our strong fields are then mainly consisted of the umbra of sunspots and our weak fields of the enhanced magnetic networks around sunspots. We calculate α and current helicity for such defined strong and weak fields separately. Note by doing so, not only we gain the opportunity to study the possible differences between weak and strong fields within active regions, but also we get a chance to learn indicated helicity properties of the global Sun if we identify our observed weak fields as the representatives of the general weak fields distributed over the whole surface.

3. Analysis and Discussion

3.1. Comparison with previous studies

Before we proceed to present our results it is useful to check our data reduction of this dataset with previous results obtained by other instruments and datasets. We select a subsample of our dataset, containing observations made between 1997 July to 2000 September, in order to compare with Pevtsov et al. (2001) where α_{best} and current helicity were also calculated for the same period of time. The difference is that their magnetograms were obtained by the Haleakala Stokes Polarimeter (HSP) at Mees Solar Observatory.

Figure 1 presents the latitudinal profile of α_{best} for the 391 active regions observed by Huairou magnetograph during this period of time. Each point presents the average value of α_{best} when multiple magnetograms of the same active region were obtained. Note in producing this figure we did not separate the weak and strong fields but instead use all data points with $|B_z| > 100G$ and $|B_x, B_y| > 200G$, in order to make a reasonable comparison with Pevtsov et al. (2001). The green line shows the least-square best-fit linear function of these α_{best} values. The similarity between our figure and Figure 1 of Pevtsov et al. (2001) indicates a good consistence between the two datasets.

Out of our 391 active regions during this period, 58.9% of 214 active regions in the northern hemisphere have $\alpha_{best} < 0$ and 67.2% of 117 active regions in the southern hemisphere have $\alpha_{best} > 0$. These numbers are consistent with the numbers of 62.9% and 69.9% for the northern and southern hemispheres respectively in Pevtsov et al. (2001). Our data shows no tendency of hemispheric rule by current helicity. 44.4% of 214 active regions in the northern hemisphere have $h_c < 0$ and 45.8% of 117 active regions in the southern hemisphere have $h_c > 0$. Note in Pevtsov et al. (2001) a much weaker tendency is also found with numbers of 50% and 57.5% for their h_c values in the northern and southern hemispheres respectively. They contribute this difference to Faraday rotation. But we suggest the difference is largely (although possibly not all) because of a physical point which we will return to address below.

Averages of α_{best} for active regions observed in each 10 degrees of solar latitudes are also plotted in Figure 1, presented as red square symbols. The large error bars of these averages remind us that our established hemispherical rule is of a statistical result. Individual active regions may present large deviations from the mean values. This is also true for other statistical results that we will present below.

3.2. Helicity observation of weak fields

Figure 2 presents our result of solar cycle variations of α (top panel) and current helicity (middle panel) for weak fields ($100G < |B_z| < 500G$). Each point in these plots is a weighted average of $\langle \alpha_z \rangle$ or current helicity for active regions observed during one year. For active regions in the southern hemisphere the weight is set to 1 and for active regions in the northern hemisphere the weight is set to -1. The weighted averages then indicate the magnitudes of α or current helicity averaged over the global surface during a whole year, assuming the northern and southern hemispheres have opposite helicity signs. We see that both averaged α and current helicity have positive signs except for the Year 2004. This tells us that both α and current helicity for weak fields obey the established hemispheric rule during most years of the solar cycle. The averaged α and current helicity for Year 2004 are negative, which indicates the usual hemispheric rule is not followed in this year. This is consistent with Hagino & Sakurai (2005) where they also found a violation of the usual hemispheric rule during solar minimums.

Figure 2 also presents a rough tendency of a decrease of α and current helicity with the development of solar cycle. We notice in Berger & Ruzmaikin (2000) the helicity production rate by differential rotation in solar interior is calculated and their calculation also shows a similar decrease of magnitudes of the rate of helicity transported into the northern and southern hemisphere respectively. This can be seen from the bottom panel of Figure 2 where the helicity transportation rate into the southern hemisphere by the m=0 mode is replotted, with data taken from Berger & Ruzmaikin (2000). This interesting consistence seems to suggest that differential rotation is the source of helicity production in solar interior although we are not able to make a conclusion because we do not know whether the α effect will also produce the same tendency or not.

As pointed out by the careful referee, the calculated transferred helicity ends at zero during solar minimums whereas our observation as well as Hagino & Sakurai (2005) show the helicity goes to the opposite sign during solar minimums. We intend to explain this as a result of trans-equatorial reconnection (Pevtsov 2000) which has consumed the helicity of the dominate sign in each hemisphere, a point interesting of itself but is out of the scope of current letter.

Another interesting implication of Figure 2 is that, whereas we usually consider helicity variation as a function of latitude as presented in Figure 1, another possibility is that the helicity variation is more associated with solar cycle dependence and the known latitude dependence is just a derived relation from this solar cycle dependence of helicity and the Butterfly diagram.

3.3. Helicity observation of strong fields

For strong magnetic fields ($|B_z| > 1000G$), calculation of weighted averages of α and current helicity presents an interesting result, shown in Figure 3. All averaged α and current helicity are negative, which means they do not follow the usual hemispheric rule. This also means that strong fields have a helicity sign opposite to that of weak fields.

As we have mentioned earlier, if we interpret our observed weak fields in active regions as the representatives of the general weak fields distributed over the global Sun, then we may use them to represent the large-scale field. Our strong fields may be used to represent the small-scale fluctuations compared to the large-scale of the global Sun. Then under this interpretation our observation seems to be consistent with the theory that solar dynamo would produce opposite helicity signs in the mean field and in the fluctuations.

It is also interesting to notice that in Berger & Ruzmaikin (2000) the higher modes helicity, such as the m=5 mode replotted in Figure 3, also has a sign opposite to that of the m=0 mode. Again, if we interpret their low-degree (such as m=0) mode field corresponds to our weak field because both of them represent a more uniformly-distributed field over the global Sun and their high-degree (such as m=5) mode field corresponds to our strong field because both of them are sporadically appeared on the surface, then their calculation and our observation show a consistence again.

The observation that strong fields have a helicity sign opposite to that of weak fields may help us understand why α_{best} usually shows a better hemispheric rule than current helicity if both quantities are calculated from vector magnetograms of the whole field (Pevtsov et al. 2001). We interpret it as follows. When we calculate α_{best} of the whole field, each data point is given an equal weight. This results in the calculated α_{best} presenting the sign of weak fields, whose number of data points dominates over that of strong fields. But when we calculate the current helicity of the whole field, defined as $h_c = B_z \cdot (\nabla \times \mathbf{B})_z = \alpha B_z^2$, we have attributed a weight of B_z^2 to each data point. This then results in a nearly cancellation of current helicity between the weak and strong fields because weak and strong fields happen to have opposite helicity signs and the former has a larger number of data points but smaller B_z^2 values for each data point whereas the latter has a smaller number of data points but each data point has a larger B_z^2 value.

It has been suggested that Faraday rotation contributes to the difference between α_{best} and current helicity. We suggest the main reason is the opposite helicity signs between weak and strong fields. J. T. Su & H. Q. Zhang (2006, in preparation) recently did a calculation and it shows that whereas Faraday rotation may rotate the transverse fields to 20 - 30 degrees, the resultant α values are less influenced, with changes of α values all less than a

few percentages. Another comment is that if Faraday rotation is the reason of the difference we should not see the difference in the dataset obtained by spectrograph-type magnetographs where the effect of Faraday rotation can be taken care of by inversion methods. But the difference is observed in Pevtsov et al. (2001) where HSP data are used. We have recently checked several active regions observed by ASP/HAO. Similar feature of opposite helicity signs between weak and strong fields is found, although not in every region examined. Also kindly pointed out by the referee, similar tendency of opposite helicity signs is also indicated in a decaying active region observed by ASP (Figure 4 of Pevtsov & Canfield 1999).

Finally we point out another consistence of our observation with previous study. By applying a known reconstruction technique to MDI data Pevtsov and Latushko (2000) calculated the current helicity of the global Sun. They found that the usual hemispheric rule is followed for regions above 40 degrees of solar latitudes whereas the rule is surprisingly not obvious for regions within 40 degrees of solar latitudes. With our observation, we now can interpret it as follows. In high latitudes magnetic fields are dominated by weak fields with their signs following the usual hemispherical rule, whereas in low latitudes strong fields with an opposite helicity sign present to result in a reduction to the usual hemispherical rule.

4. Summary

A large sample of 17200 photospheric vector magnetograms of active regions obtained from January 1997 to August 2004 is analyzed in this letter. Different from other works, we calculate the helicity proxies, α and current helicity, for weak ($100G < |B_z| < 500G$) and strong ($|B_z| > 1000G$) fields separately.

By analyzing this dataset we find that: 1. For weak magnetic fields, the signs of both α and current helicity follow the established hemispheric rule except during the Year 2004. The magnitudes of their weighted averages show a weak tendency of decreasing with the development of solar cycle. 2. For strong magnetic fields, both α and current helicity show a helicity sign opposite to that of weak fields.

Our results seem to be consistent with the theoretical prediction that solar dynamo would produce opposite helicity signs in the mean field and in the fluctuations as well as the theoretical calculations of helicity production rate by differential rotation. However, as pointed out by the referee, some previous studies (Longcope et al. 1998,1999; Chae 2001) have suggested that neither the interface dynamo nor the differential rotation would generate sufficient amount of helicity (twist). So our observation with its interesting implications advocates further investigations, both observationally and theoretically.

I thank Mitchell Berger for providing his calculation data used in the letter. I also thank the anonymous referee for helpful comments and suggestions. This work was supported by the One-Hundred-Talent Program of the Chinese Academy of Sciences, the Chinese National Science Foundation under Grant 10373016, and the U.S. National Science Foundation under Grant ATM-0548060.

REFERENCES

Ai, G., Li, W., Zhang, H. 1982, Chinese Astronomy and Astrophysics, 6, 129

Ai, G., Hu, Y. 1986, Acta Astron. Sin, 27, 173

Bao, S., Zhang, H. Q. 1998, ApJ, 496, L43

Berger, M. A. 1984, Geophys. Astrophys. Fluid Dynamics, 30, 79

Berger, M. A., Field, G. B. 1984, J. Fluid Mech., 147, 133

Berger, M. A., Ruzmaikin, A. 2000, J. Geophys. Res., 105, 10481

Blackman, E. G., Field, G. B. 2000, MNRAS, 318, 724

Burnette, A. B., Canfield, R. C., Pevtsov, A. A. 2004, ApJ, 606, 565

Chae, J. 2001, ApJ, 560, L95

Demoulin, P., et al. 2002, A&A, 382, 650

Hagino, M., Sakurai, T. 2005, PASP, 57, 481

Kurokawa, H. 1987, Sol. Phys., 113, 259

Leka, K. D., Canfield, R. C., McClymont, A. N., van Driel-Gesztelyi, L. 1996. ApJ, 462, 547

Longcope, D. W., Fisher, G. H., Pevtsov, A. A. 1998, ApJ, 507, 417

Longcope, D. W., Linton, M., Pevtsov, A. A., et al. 1999, in *Magnetic Helicity in Space and Laboratory Plasma*, Geophysical Monograph 111, ed. M. R. Brown, R. C. Canfield, A. A. Pevtsov, p.93

Low, B. C. 2001, J. Geophys. Res., 106, 25141

Moffatt, H. K. 1985, J. Fluid Mech., 159, 359

Ossendrijver, M. 2003, Astron. Astrophys. Rev., 11, 287

Pevtsov, A. A. 2000, ApJ, 531, 553

Pevtsov, A. A., Canfield, R. C. 1999, in *Magnetic Helicity in Space and Laboratory Plasma*, Geophysical Monograph 111, ed. M. R. Brown, R. C. Canfield, A. A. Pevtsov, p.103

Pevtsov, A. A., Canfield, R. C., Latushko, S. M. 2001, ApJ, 549, L261

Pevtsov, A. A., Canfield, R. C., Metcalf, T. R. 1994, ApJ, 425, L117

Pevtsov, A. A., Canfield, R. C., Metcalf, T. R. 1995, ApJ, 440, L109

Pevtsov, A. A., Latushko, S. M. 2000, ApJ, 528, 999

Zhang, H. Q., Ai, G. X. 1986, Acta Astron. Sin., 27, 217

Zhang, M., Low, B. C. 2005, ARAA, 43, 103

Zhang, M., Flyer, N., Low, B. C. 2006, ApJ, 644, 575

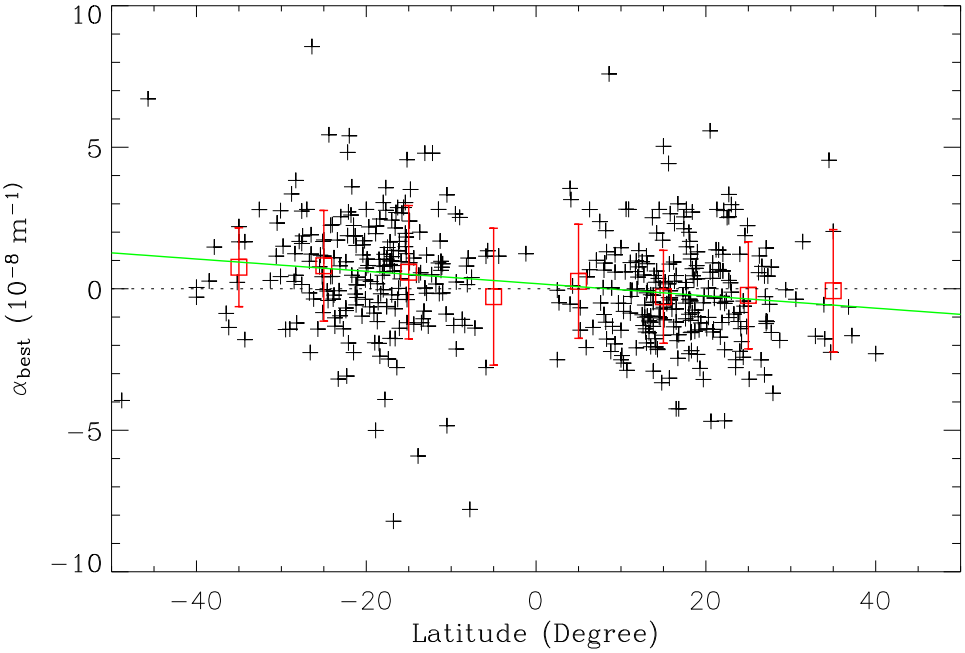

Fig. 1.— Latitudinal profile of α_{best} for the 391 active regions observed by Huairou magnetograph between 1997 July and 2000 September.

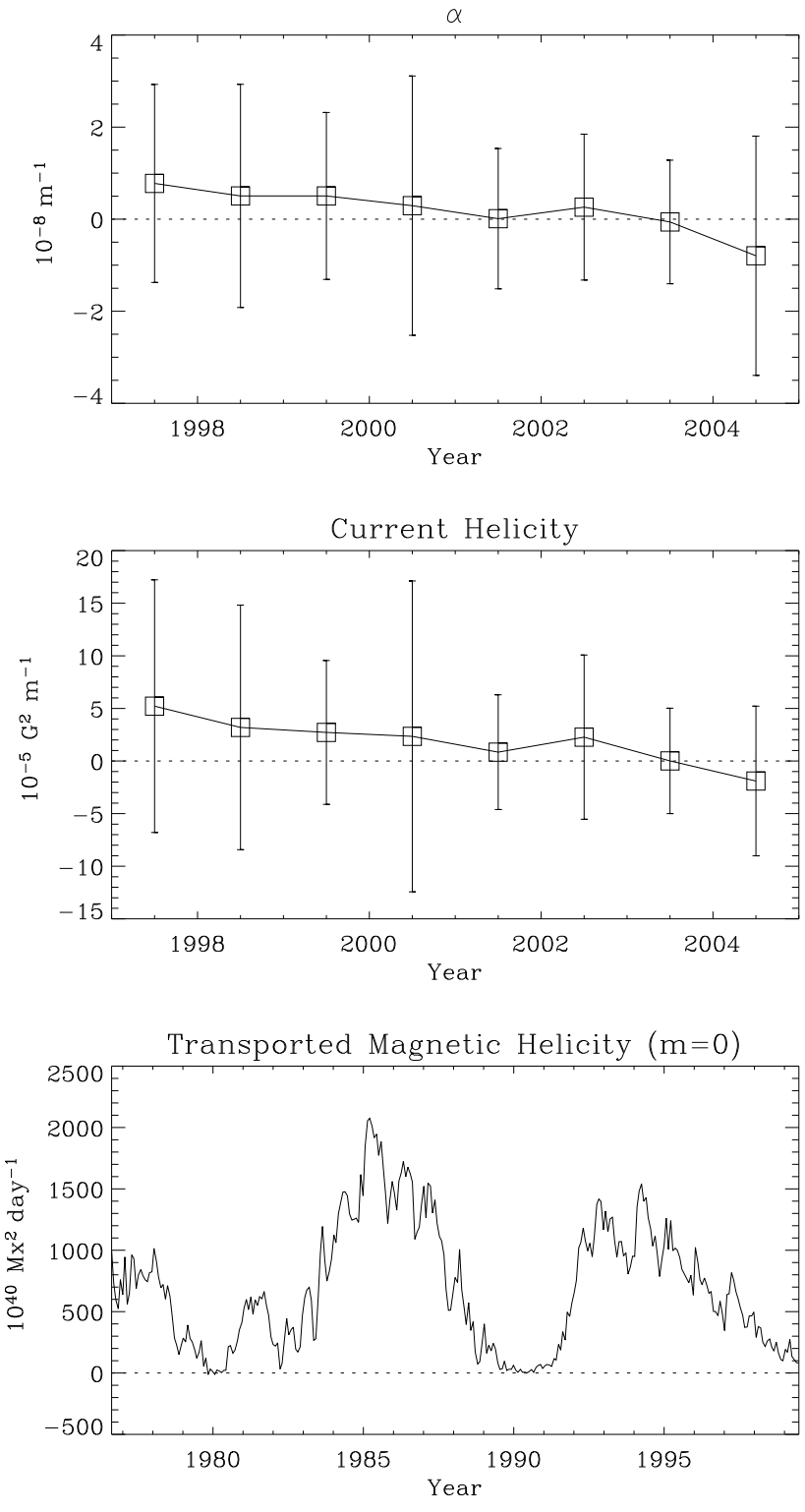

Fig. 2.— Solar cycle variations of weighted averages of α (top panel) and current helicity (middle panel) for weak fields ($100G < |B_z| < 500G$). Bottom panel: Calculated transfer rate of $m = 0$ mode helicity, created by differential rotation in the interior, into the southern hemisphere. Adopted from Berger & Ruzmaikin (2000).

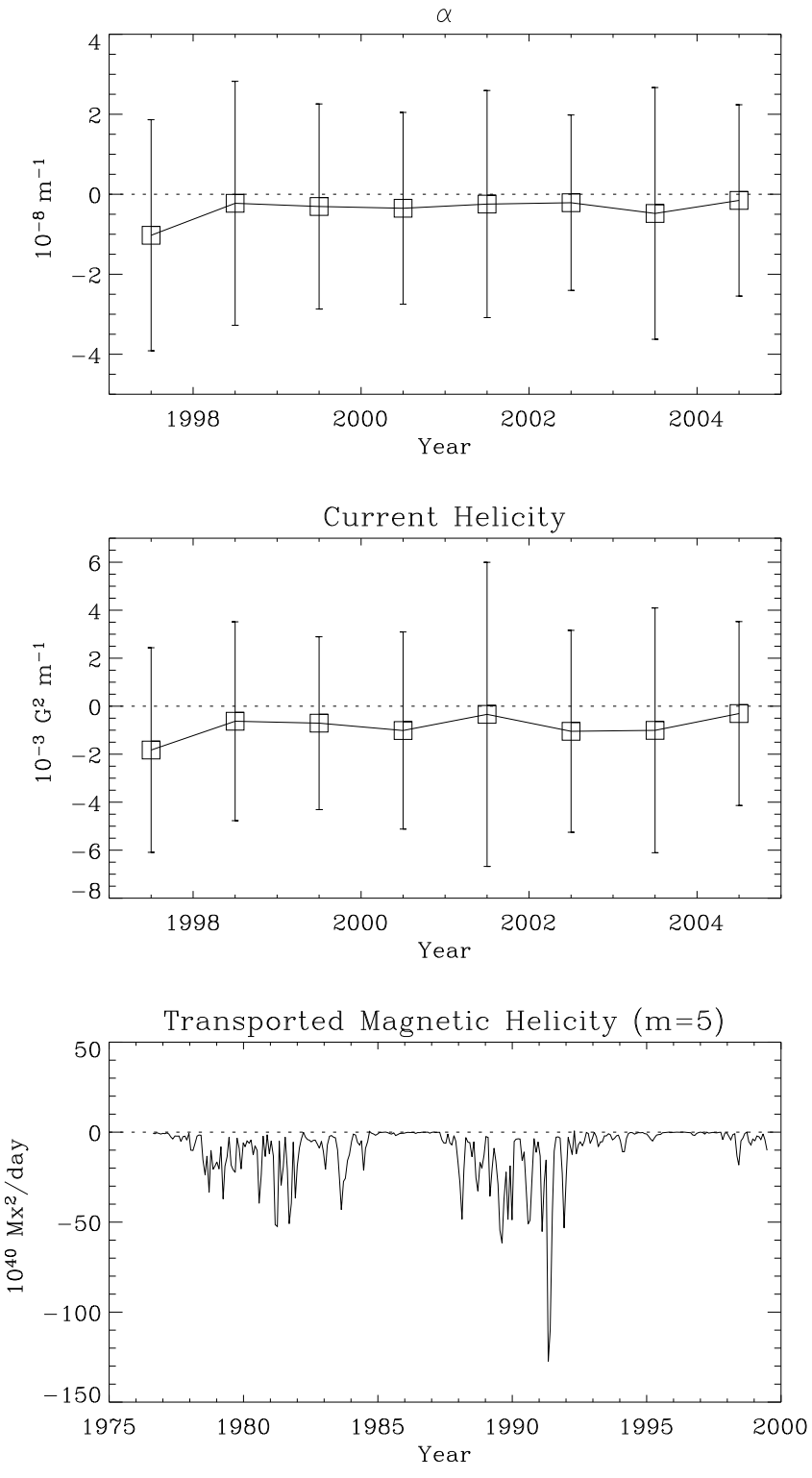

Fig. 3.— Top and middle panels: Same as in Figure 2 but for strong fields ($|B_z| > 1000G$). Bottom panel: Same as in Figure 2 but for $m = 5$ mode.